# First Measurement of the Velocity of Slow Antihydrogen Atoms

G. Gabrielse,[1,*] A. Speck,[1] C. H. Storry,[1] D. LeSage,[1] N. Guise,[1] D. Grzonka,[2] W. Oelert,[2] G. Schepers,[2] T. Sefzick,[2]
H. Pittner,[3] J. Walz,[3] T. W. Hänsch,[3,4] D. Comeau,[5] and E. A. Hessels[5]

(ATRAP Collaboration)

[1]*Department of Physics, Harvard University, Cambridge, Massachusetts 02138, USA*
[2]*IKP, Forschungszentrum Jülich GmbH, 52425 Jülich, Germany*
[3]*Max-Planck-Institut für Quantenoptik, Hans-Kopfermann-Strasse 1, 85748 Garching, Germany*
[4]*Ludwig-Maximilians-Universität München, Schellingstrasse 4/III, 80799 München, Germany*
[5]*York University, Department of Physics and Astronomy, Toronto, Ontario M3J 1P3, Canada*
(Received 31 March 2004; published 10 August 2004)

The speed of antihydrogen atoms is deduced from the fraction that passes through an oscillating electric field without ionizing. The weakly bound atoms used for this first demonstration travel about 20 times more rapidly than the average thermal speed of the antiprotons from which they form, if these are in thermal equilibrium with their 4.2 K container. The method should be applicable to much more deeply bound states, which may well be moving more slowly, and should aid the quest to lower the speed of the atoms as required if they are to be trapped for precise spectroscopy.

When the goal of producing "cold" antihydrogen ($\overline{\text{H}}$) was laid out long ago [1], the objective was $\overline{\text{H}}$ atoms that were cold enough to be confined in a neutral particle trap for precise spectroscopy and gravitation studies. This stringent definition of "cold" requires $\overline{\text{H}}$ energies significantly below the 0.5 K depth of superconducting magnetic traps, when these are placed in the $\sim 1$ Tesla bias field needed to confine the antiprotons ($\overline{p}$) and positrons ($e^+$) for $\overline{\text{H}}$ production.

Antihydrogen produced during the positron cooling of antiprotons [2] in a nested Penning trap [3] was called "cold" antihydrogen in reports of its observation [4–6]. However, no $\overline{\text{H}}$ energy, velocity, or temperature was actually measured. The observed atoms were clearly cold compared to $\overline{\text{H}}$ moving at nearly the speed of light [7,8]. Almost certainly the $\overline{\text{H}}$ energy was less than the tens of eV well depths of the potential wells used to confine the $\overline{p}$ and $e^+$ from which the $\overline{\text{H}}$ were formed. It was naturally hoped that the $\overline{\text{H}}$ were in thermal equilibrium with the 4.2 K [5,6] or 15 K [4] temperature of the electrodes confining the $\overline{p}$ and $e^+$.

In this Letter we report the first measurement of the velocity of $\overline{\text{H}}$ atoms. The change in $\overline{\text{H}}$ transmission efficiency through an oscillating electric field is measured as a function of the field's oscillation frequency. ATRAP's background-free field ionization detection method [5] registers only $\overline{\text{H}}$ that reach the detection well intact. Atoms moving slowly enough will never make it through the electric field without being ionized. Faster atoms are sometimes able to pass while the oscillating field is too weak to ionize them, depending upon the phase of the field. In this first demonstration we deduce that the most weakly bound $\overline{\text{H}}$ that we detect have an energy that is about 200 meV, a speed that is about 20 times higher than

an average thermal speed at 4.2 K. More deeply bound $\overline{\text{H}}$ observed to survive a 360 V/cm electric field may move more slowly; this method should make it possible to check, though the measurements will take much more time than has been available so far. No attempt has yet been made to minimize the $\overline{p}$ driving forces that bring $\overline{p}$ and $e^+$ into repeated contact [6].

The ATRAP apparatus is represented in Fig. 1, with a cross section of the crucial volume in Fig. 2(a). In preparation for $\overline{\text{H}}$ production, typically $2 \times 10^5$ $\overline{p}$ from CERN's Antiproton Decelerator are accumulated for this demonstration. The well-established techniques for slowing, trapping, cooling, and stacking [9,10] are now used in all $\overline{\text{H}}$ experiments. The $\overline{p}$ cool by collisions to equilibrium with trapped, 4.2 K electrons. (The electrons
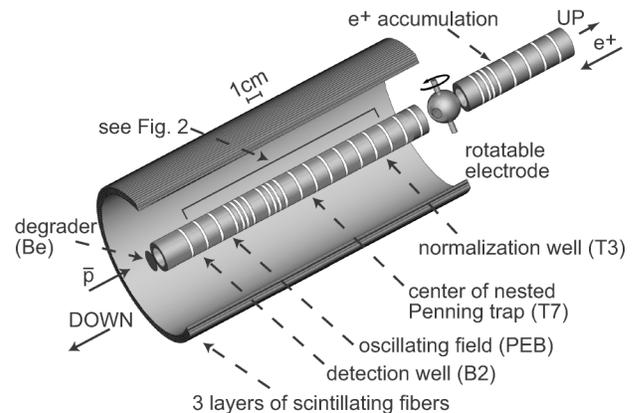


FIG. 1. Antiprotons are loaded from below (left), into the trap electrodes below the rotatable electrode. Positrons are simultaneously loaded from above (right) into the electrodes above the rotatable electrode.
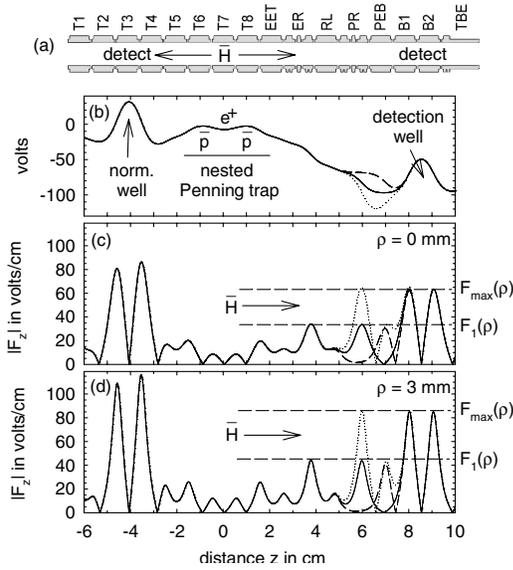
FIG. 2.   Cross section of trap electrode (a), potential on axis
(b) and the magnitude of the axial electric field on axis (c) and
3 mm off axis (d). Solid curves are the static potentials and
axial electric fields magnitudes. Dashed and dotted curves
show the maximum variation of these when the oscillating
potential is added.

cool via synchrotron radiation to thermal equilibrium
with the 4.2 K trap electrodes.) The $\overline{p}$ are then positioned
in the side wells of a nested Penning trap [Fig. 2(b)] by
manipulating the potentials applied to the vertical stack
of ring electrodes. A magnetic field, $B\hat{\mathbf{z}}$ with $B = 5.2$ T ,
is parallel to trap axis. Typically $4 \times 10^5 e^+$ are accumu-
lated at the same time as the $\overline{p}$ [11]. They are then posi-
tioned in the center of the nested Penning trap [Fig. 2(b)],
between the side wells for antiprotons. Like the electrons
they cool to 4.2 K by radiating synchrotron radiation.

$\overline{H}$ atoms are produced near the center of the nested
Penning trap, at the location of electrode T7 as indicated
by "$\overline{H}$" in Fig. 2(a). $\overline{H}$ atoms are produced when the $\overline{p}$ are
driven from one side well [Fig. 2(b)], by a radiofrequency
driving force, through the $e^+$ [6]. The $\overline{p}$ that do not form
$\overline{H}$ get more chances when they are driven back and forth
from one well to the other. The drives give $\overline{p}$ velocities
along the axis of the trap, either in the direction of the
normalization well or in the direction of the detection
trap. (Likely such weakly driven $\overline{H}$ production can pro-
duce slower atoms than those produced by injecting
higher energy $\overline{p}$ into a nested Penning trap for cooling
[4,5].) If an $\overline{H}$ is formed before the $e^+$ completely cool the
$\overline{p}$, then the $\overline{H}$ will have a residual axial velocity that is
larger than the average thermal velocity of the $\overline{p}$ at the
4.2 K temperature of the $e^+$ awaiting $\overline{H}$ production.

Atoms traveling in the $-\hat{\mathbf{z}}$ direction travel along the
magnetic field axis to the normalization well [Fig. 2(b)].
No potentials or fields are varied along this trajectory.
The $\overline{H}$ ionized by the strong electric fields in this well
[Figs. 2(c) and 2(d)] leave their $\overline{p}$ in the well for back-

ground free detection. This well is emptied at a later time
and the $\overline{p}$ annihilations are detected in surrounding
scintillators. We use this count to normalize all other $\overline{H}$
measurements, thereby reducing the effect of variations
in the $\overline{H}$ production due to slightly different numbers of
$\overline{p}$ and $e^+$.

Atoms traveling in the $\hat{\mathbf{z}}$ direction will be similarly
counted in the detection well [Fig. 2(d)] if they are not
ionized by the electric field they pass through on their
way to this well. An atom will ionize if the magnitude of
the axial electric field it encounters along its trajectory
exceeds a value $F$ which is directly related to the size of
its internal orbit [12]. The field along an $\overline{H}$ trajectory
always has a static component $F_{dc}(\rho, z)\hat{\mathbf{z}}$, and we can
add a time varying axial field $F_{ac}(\rho, z)\cos(\omega t + \phi)\hat{\mathbf{z}}$.

While we can only measure the number of $\overline{H}$ atoms that
travel into the very small solid angle of our detection
well, a simple example gives clear evidence that driven $\overline{H}$
production sends $\overline{H}$ preferentially directed along the mag-
netic field axis, $\pm\hat{\mathbf{z}}$. From $4.5 \times 10^6$ $e^+$ and $2.9 \times 10^5$ $\overline{p}$
we detect $7.6 \times 10^3$ $\overline{H}$ in the detection and normalization
wells. Since the combined solid angle of the detection and
normalization wells is less than $4\pi/100$, the $\overline{H}$ production
cannot be isotropic since several times more $\overline{p}$ would be
required than the number available.

A measurement of the $\overline{H}$ velocity is very simple in
principle. With the oscillating field turned off, the ratio
of $\overline{H}$ atoms ionized in the detection and normalization
wells is obtained (open square in Fig. 3). This point has no
frequency associated with it, but is plotted on the same
vertical scale as the other points on the graph. These come
from measurements with the oscillating field turned on,
for different values of oscillation frequency $\omega/(2\pi)$ (solid
points in Fig. 3). The fraction of $\overline{H}$ atoms detected de-
creases as $\omega$ increases. As $\omega$ increases, fewer atoms travel
quickly enough through the oscillating field to avoid
ionization, and fewer atoms are thus detected. The $\overline{H}$
atoms are produced under the same conditions for each
measurement, and the count from the detection well is
normalized as discussed above. Electric field gradients
can change the speed of a highly excited and polarizable
$\overline{H}$ atom, but this is a small affect here since the preioniz-
ing field is relatively spatially uniform [12].

The vertical scale for Fig. 3 is chosen so that the
measurement with no oscillating field is consistent with
1, and so that the measured $\omega \to 0$ limit of the oscillating
field measurements is consistent with 0.62. The latter is
the fraction of the time that the magnitude of the oscil-
lating electric field, along the trajectory of an $\overline{H}$ traveling
to the detection well, is less than the maximum static field
along this path. In this limit 0.62 of all the $\overline{H}$ traveling to
the detection well should thus not be ionized by the
oscillating field.

To interpret our measurements quantitatively we consi-
der the $N(\rho, v, F)d\rho dv dF$ antihydrogen atoms produced
at $z = 0$ and $t = 0$, at a radius between $\rho$ and $\rho + d\rho$,
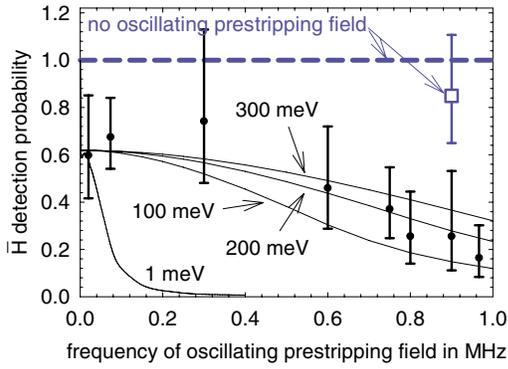with an axial velocity between $v$ and $v + dv$, and which

FIG. 3 (color online). The fraction of the $\overline{H}$ atoms detected in the detection well decreases as the frequency $\omega/(2\pi)$ of the oscillating electric field is increased (solid points). More atoms are detected when there is no oscillating field (open square). This point is plotted on the same scale as the others but it has no frequency associated with it. The measured points are compared to a simple model discussed in the text; the solid curves apply when the oscillating electric field is applied, and the dashed curve when it is not.

are in a state that will be ionized by an axial electric field between $F$ and $F + dF$.

When no time varying electric field is applied, the $\overline{H}$ atoms on their way to the detection well experience an axial electric field $F_{dc}(\rho, z = vt)$. Figure 2 shows $F_{dc}(\rho, z)$ for $\rho = 0$ (c) and $\rho = 3$ mm (d), along with the corresponding values $F_1(\rho = 0) = 34$ V/cm and $F_1(\rho = 3 \text{ mm}) = 45$ V/cm. The number of detected $\overline{H}$ is thus

$$N_o = \int_0^{\rho_{max}} d\rho \int_0^\infty dv \int_{F_1(\rho)}^{F_{max}(\rho)} dF N(\rho, v, F). \quad (1)$$

Detected atoms are those that ionize between $F_1(\rho)$ and $F_{max}(\rho)$, the maximum values of $F_{dc}(\rho, z)$ that they encounter before and within the detection well, respectively.

When the alternating axial electric field, $F_{ac}(\rho, z) \times \cos(\omega t + \phi)$, is applied the $\overline{H}$ atoms traveling towards the detection well encounter a net axial field

$$F(\rho, z, \omega/v, \phi) = F_{dc}(\rho, z) + F_{ac}(\rho, z) \cos\left(\frac{\omega z}{v} + \phi\right), \quad (2)$$

where we must later average over all phases $\phi$. The number of detected $\overline{H}$ is

$$N = \int_0^{\rho_{max}} d\rho \int_0^\infty dv \int_0^{2\pi} \frac{d\phi}{2\pi} \int_{F_2(\rho,\omega/v,\phi)}^{F_{max}(\rho)} dF N(\rho, v, F). \quad (3)$$

The limit $F_2(\rho, \omega/v, \phi)$ is the maximum axial field magnitude (i.e., the maximum $|F(\rho, z, \omega/v, \phi)|$) that an $\overline{H}$ sees at any $z$ before the detection well begins.

We make the simplest assumption—that the $\overline{H}$ are produced uniformly out to a radius $\rho_{max} = 3$ mm—approximately the measured extent of our $e^+$ plasma [13]. (Later we show that we are not very sensitive to this

assumption.) We also assume the measured power law dependence $N \sim F^{-3}$ [14]. Finally we assume that the $\overline{H}$ have a velocity $v_o\hat{z}$, since we expect that driven $\overline{H}$ production produces atoms traveling along the magnetic field direction. We would expect the same result for any velocity spread that is narrow compared to the average velocity. Thus

$$N(\rho, v, F) \sim \frac{2\pi\rho}{\pi\rho_{max}^2} \delta(v - v_o) F^{-3}. \quad (4)$$

The solid curves in Fig. 3 show the fraction of $\overline{H}$ atoms that should be detected when the oscillating electric field is turned on, for various values of the $\overline{H}$ kinetic energy $\frac{1}{2}Mv_o^2$, where $M$ is the $\overline{H}$ mass.

An $\overline{H}$ kinetic energy of 200 meV is a good fit to our measurements (2400 K in temperature units). This conclusion is rather insensitive to our assumptions. For example, if we had assumed that all the $\overline{H}$ was produced on the central axis, then we would have concluded that the $\overline{H}$ velocity was about 100 meV. If we had instead assumed that all the $\overline{H}$ was produced 4 mm off axis, then we would have concluded that the $\overline{H}$ velocity was 300 meV. A 200 meV $\overline{H}$ velocity is much higher than the 0.3 meV average energy for a 4.2 K thermal distribution—the lowest possible average $\overline{p}$ and $\overline{H}$ energy. Even the 1 meV curve in Fig. 3 is far from consistent with our data.

An electric field gradient $\partial F_z/\partial z$ exerts a force on a highly polarizable $\overline{H}$ [12]

$$f_z = \frac{e^2\rho^3}{2r_e m_e c^2} \frac{\partial[F_z(z)^2]}{\partial z}. \quad (5)$$

Here $e$ is the proton charge, $\rho$ is the radial size of the $\overline{H}$ atom, $r_e$ is the classical electron radius, and $m_e c^2$ is the electron rest energy. For fields nearly strong enough to ionize the atom the force increases beyond this value. We use the overestimates $F_z = 100$ V/cm and a gradient $\partial F_z/\partial z = 100$ V/cm$^2$ applied over 1 cm, together with the size $\rho = 0.3$ $\mu$m of the largest atom that survives $F_{dc} = 40$ V/cm. The resulting force would change the velocity of a 200 meV $\overline{H}$ by less than a percent, justifying the neglect of the gradient force on a polarized $\overline{H}$ in this work. For lower $\overline{H}$ speeds more care must be taken.

For a $\overline{p}$ traveling in the $\hat{z}$ direction through the $e^+$ plasma, one $\overline{p}$ speed that seems important is the one that equals the average axial speed of the $e^+$ that are going in the same direction as the $\overline{p}$. For 4.2 K $e^+$ this corresponds to a $\overline{p}$ energy of 210 meV. This is close to what we measure, likely by coincidence given the approximate character of the estimate. One might expect increased $\overline{H}$ production at this $\overline{p}$ energy, but this depends in a complicated way upon how quickly the $\overline{p}$ are being cooled by the $e^+$. A recombination rate that depends upon the relative velocity of the $\overline{p}$ and $e^+$ will become insensitive to $\overline{p}$ energies below this value, since the relative velocity will be determined by the $e^+$ velocity.

Another important speed is

$$v_p = n_e(\pi b^2)v_e L. \tag{6}$$

This $\overline{p}$ speed would allow just enough time in the $L \approx$ 1 mm thick $e^+$ plasma for there to be a deexcitation collision [15] between the $e^+$ initially picked up by the $\overline{p}$ and another $e^+$ in the plasma on average. The expected $e^+$-$e^+$ collision rate should be of order $n_e(\pi b^2)v_e$ where $n_e = 1.6 \times 10^7/\text{cm}^3$ is the $e^+$ density and $v_e$ is the average thermal speed for a $e^+$ at $T_e = 4.2$ K. The distance of closest approach $b$ comes from equating the potential energy $(4\pi\epsilon_o)^{-1}e^2/b$ and the thermal energy $kT_e$. The corresponding $\overline{p}$ energy, and hence the $\overline{\text{H}}$ energy, is 460 meV—larger than we observe. The cross section used is only an estimate, of course, and the $e^+$ may be heated some by the $\overline{p}$. Notice that $v_p \propto n_e L T_e^{-3/2}$, suggesting that a $e^+$ plasma with a lower density, a shorter length and a higher temperature will produce $\overline{\text{H}}$ with lower velocities.

The relatively high velocities that we observe may also be related to the fact that this first demonstration experiment measures only the speed of the most weakly bound $\overline{\text{H}}$ states, which may have had less cooling time. Because the number of $\overline{\text{H}}$ atoms detected goes down steeply as the strength of the ionization field $F$ is increased, as $F^{-3}$ [14], the $\overline{\text{H}}$ atoms that we detect are essentially all atoms which will ionize just above the maximum static electric field $[F_1(\rho)]$ in the region before the detection well.

More deeply bound $\overline{\text{H}}$ states may well have much lower velocities if these arise because of more collisions of the $\overline{\text{H}}$ with $e^+$ in the plasma. It should be possible to use this new technique to measure the velocity of more deeply bound states. The experiment is simple in principle. The deeply bound states can be selected by raising the maximum value $F_1(\rho)$ of the static electric field $F_{dc}(\rho, z)$. The challenge in practice is that the number of deeply bound states observed goes down inversely as the cube of this field value, greatly increasing the time required to accumulate data.

In conclusion, a new method makes it possible to measure the speed of slow $\overline{\text{H}}$ atoms for the first time. For the most weakly bound states, our measurements fit well to a 200 meV $\overline{\text{H}}$ energy. This is close to the estimated 210 meV $\overline{\text{H}}$ energy below which the $\overline{\text{H}}$ formation rate no longer increases. It is lower than the 460 meV energy that is estimated to allow a deexcitation collision between the $e^+$ in an $\overline{\text{H}}$ and a $e^+$ in the surrounding plasma on average. It is higher than the lowest possible energy, the 0.3 meV average energy of a 4.2 K thermal distribution of H.

The new method should reveal how the $\overline{\text{H}}$ velocity depends upon the strength of the driving force, the number and density of the $e^+$ and $\overline{p}$, and upon the binding energy or size of the $\overline{\text{H}}$ atoms. Slowly lowering the depth of the center well in the nested Penning trap may produce slower $\overline{\text{H}}$, as may interchanging the position of the $e^+$ and $\overline{p}$ in this trap. The first step towards devising ways to get the coldest possible $\overline{\text{H}}$ atoms, of course, is a method to measure the $\overline{\text{H}}$ speed, which is now available.

*Corresponding author.
Electronic address: gabrielse@physics.harvard.edu

[1] G. Gabrielse, in *Fundamental Symmetries*, edited by P. Bloch, P. Paulopoulos, and R. Klapisch (Plenum, New York, 1987), pp. 59–75.

[2] G. Gabrielse, J. Estrada, J. N. Tan, P. Yesley, N. S. Bowden, P. Oxley, T. Roach, C. H. Storry, M. Wessels, J. Tan, D. Grzonka, W. Oelert, G. Scheppers, T. Sefsick, W. Breunlich, M. Carngelli, H. Fuhrmann, R. King, R. Ursin, H. Zmeskal, H. Kalinowsky, C. Wesdorp, J. Walz, K. S. E. Eikema, and T. Haensch, Phys. Lett. B **507**, 1 (2001).

[3] G. Gabrielse, S. L. Rolston, L. Haarsma, and W. Kells, Phys. Lett. A **129**, 38 (1988).

[4] M. Amoretti *et al.*, Nature (London) **419**, 456 (2002).

[5] G. Gabrielse, N. S. Bowden, P. Oxley, A. Speck, C. H. Storry, J. N. Tan, M. Wessels, D. Grzonka, W. Oelert, G. Schepers, T. Sefzick, J. Walz, H. Pittner, T. W. Hänsch, and E. A. Hessels, Phys. Rev. Lett. **89**, 213401 (2002).

[6] G. Gabrielse, N. S. Bowden, P. Oxley, A. Speck, C. H. Storry, J. N. Tan, M. Wessels, D. Grzonka, W. Oelert, G. Schepers, T. Sefzick, J. Walz, H. Pittner, T. W. Hänsch, and E. A. Hessels, Phys. Rev. Lett. **89**, 233401 (2002).

[7] G. Baur, G. Boero, S. Brauksiepe, A. Buzzo, W. Eyrich, R. Geyer, D. Grzonka, J. Hauffe, K. Kilian, M. L. Vetere, M. Macri, M. Moosburger, R. Nellen, W. Oelert, S. Passagio, A. Pozzo, K. Rohrich, K. Sachs, G. Schepers, T. Sefzick, R. Simon, R. Stratmann, F. Stinzing, and M. Wolke, Phys. Lett. B **368**, 251 (1996).

[8] G. Blanford, D. C. Christian, K. Gollwitzer, M. Mandelkern, C. T. Munger, J. Schultz, and G. Zioulas, Phys. Rev. Lett. **80**, 3037 (1998).

[9] G. Gabrielse, Adv. At. Mol. Opt. Phys. **45**, 1 (2001).

[10] G. Gabrielse, N. S. Bowden, P. Oxley, A. Speck, C. H. Storry, J. N. Tan, M. Wessels, D. Grzonka, W. Oelert, G. Schepers, T. Sefzick, J. Walz, H. Pittner, and E. Hessels, Phys. Lett. B **548**, 140 (2002).

[11] J. Estrada, T. Roach, J. N. Tan, P. Yesley, and G. Gabrielse, Phys. Rev. Lett. **84**, 859 (2000).

[12] D. Vrinceanu, B. E. Granger, R. Parrott, H. R. Sadeghpour, L. Cederbaum, A. Mody, J. Tan, and G. Gabrielse, Phys. Rev. Lett. **92**, 133402 (2004).

[13] P. Oxley *et al.* Phys. Lett. B **595**, 60 (2004).

[14] G. Gabrielse *et al.* (to be published).

[15] M. Glinsky and T. O'Neil, Phys. Fluids B **3**, 1279 (1991).